Combined impact of power take-off capping and of wave resource description on wave energy converter performance

Lissie M de la Torre-Castro, Rémy Claude René Pascal, Yves Perignon, Aurélien Babarit, Grégory S Payne

Combined impact of power take-off capping and of wave resource description on wave energy converter performance

de la Torre - Castro, L.M.[a], Pascal, R.C.R.[b], Perignon, Y.[a], Babarit, A.[a], Payne, G.S.[a,1,*]

[a] *LHEEA, Ecole Centrale de Nantes and CNRS (UMR6598), Nantes, FR*
[b] *INNOSEA Ltd, Floor 2, Murchinson house, 10 Max Born Crescent, Edinburgh, EH9 3BF, UK*

Abstract

Wave energy converters (WECs) energy production estimates are key metrics for performance predictions. This study compares four methods for energy production assessment: power matrix, interpolated power matrix, capture length matrix and a reference method based on the exact omnidirectional spectra for every sea state. Two deployment sites are considered and their wave resource is derived from hindcast databases. The WEC chosen for this study is a two-body self-referenced heaving device characterised using a boundary element method (BEM) numerical model run in time-domain and accounting for some non-linearities. The model also includes power take-off capping, in terms of power capacity and a force cap, independently. A novel metric is introduced to assess the shape similarity between two spectra and it is used to assess the impact of approximating raw spectra with standard ones on energy production estimates. The study shows that the power take-off capping approaches and values and the way the exact resource spectra are approximated have a significant impact WEC energy estimation methods accuracy. Indeed, relative differences in yearly production estimates with respect to the benchmark method vary from 2.4% to 8.3% across capping values and estimation methods. It also shows that there is little difference in yearly averaged energy production estimates between the different "matrix based" methods. These differences are of the order of tens of percent for a given power take-off capping configuration and a given site.

Keywords: wave energy, energy production estimates, power take-off capping, wave resource characterisation
PACS: 0000, 1111
2000 MSC: 0000, 1111

1. Introduction

Ocean waves represent a large untapped source of renewable energy [1]. However, the technologies to harvest wave energy still require further maturation to become economically competitive for mainstream energy markets. One of the key metrics to assess the economical viability of

*Corresponding author
Email addresses: Lissie-Marcela.De-La-Torre-Castro@eleves.ec-nantes.fr (de la Torre - Castro, L.M.), remy.pascal@innosea.fr (Pascal, R.C.R.), yves.perignon@ec-nantes.fr (Perignon, Y.), aurelien.babarit@ec-nantes.fr (Babarit, A.), gregory.payne@farwind-energy.fr (Payne, G.S.)
[1] Present address: Farwind Energy, 1 rue de la Noë, 44300, Nantes, France

a wave energy converter (WEC) concept is its associated cost of energy. This is underpinned by the assessment of the capital expenditures (CAPEX) costs and operational expenditures (OPEX) costs of the concept and by its Annual Energy Production (AEP) estimate at the site considered, which is the focus of the present study.

The two key elements influencing WEC production estimates are the description of the wave energy resource and characterisation of the behaviour of the device (which includes the hydrodynamic properties of the WEC, its power take-off (PTO) characteristics, and the control strategy applied) in those wave conditions. At concept stage, the latter usually relies on numerical modelling and/or experimental testing, while the former can be based on hindcast modelling or on in situ measurements.

In the present study, we investigate the influence of the way the wave resource is described on energy production estimates. We also look at how the capping of the PTO mechanism, in terms of maximum power capacity and more realistically, in terms of maximum force, influences those estimates for different wave resource description techniques. The WEC considered for this study is a generic version of the WaveBob, an omni-directional device developed by the now defunct Irish company bearing the same name [2]. This device is a free-floating two-body heaving converter. It is self-reacting and can be considered as omnidirectional because of its axisymmetric design. The hydrodynamics of the wave-structure interactions are studied using linear potential flow theory; however, the numerical model runs in the time domain and non-linearities related to viscous effects and to the end stop forces of the PTO mechanism are taken into account.

Two sites are considered for the deployment of the device: a location off the French West Coast, and the more energetic Irish Belmullet testing site, off the West coast of Ireland. The wave resource description for both sites is based on spectral hindcast databases, which provide directional and spectral description of sea states at the selected locations with an hourly resolution.

This work is a continuation of two studies presented in [3] and [4]. The first one was based on a simple frequency domain modelling of a WEC with sea state characterisations inferred from in situ buoy measurements. In the second one, the power performance of the same WEC as the one considered for the current study, with an idealised power cap, was analysed. Three methods were compared to estimate the power production, and it was found out that the ones based on scatter diagrams and Joint North Sea Wave Project (JONSWAP) generated spectra overestimate the annual power production compared to the use of actual spectra. Over the years, several studies have looked at the different aspects of WEC annual energy production estimates. The following is a sample of significant contributions which have contributed to the state-of-the-art on the subject.

Early work investigating the characterisation of sea states for wave energy applications specifically can be found in [5, 6, 7]. These studies explore different methods to represent sea states (including integral parameters and spectra) and comment on their respective drawbacks and merits. [6] focuses only on wave resource representation, without investigating its impact on WECs energy production estimates. [7] provides some indications of significant variability in the power produced by a prototype, associated with sea state spectral shapes. The study however, does not assess the long-term impact of the variability on annual energy production but recommends taking into account spectral shape and not only integral parameters. The method for sea state

representation developed in [8] relies on the division of complex sea states into simpler "sub-sea states", the characterisation of which is based on integral parameters. The case study used to illustrate this method is based on the numerical modelling of the SEAREV WEC. The results show that for some sea states, energy production estimates can differ significantly between the methods used to describe them. However, as for [7], no long-term impact on the SEAREV power production is provided. [9] is an in-depth study on how the wave resource definition can affect annual energy production estimates. It considers three different WECs and four different deployment sites. The investigation is based on linear frequency domain numerical modelling. The study shows that the variability in production estimates based on different representations of the wave resource is significant. It also shows the impact of the site considered on this variability. In particular, the site exhibiting a significant proportion of multi-modal sea states is associated with high production estimate variability across the wave resource characterisation methods explored. The study presented in [10] investigates the difference in power production estimates for an omnidirectional point absorber type WEC between a spectral description of the resource and one based on the JONSWAP fit associated with the corresponding integral parameters. It concludes that the latter approach only slightly overestimates power production on average. The numerical model used in this study is based on a simple frequency domain approach. [11] presents an interesting investigation where the impact of both the type of numerical modelling used and the way the wave resource is characterised are explored. The two types of numerical modelling considered are linear frequency domain and an innovative technique defined as non-linear frequency domain, but which does not account for end stop phenomena. The resource is described either as scatter diagrams or using spectra from in-situ buoy measurements. Two types of WEC and two deployment sites are considered. The study concludes that in high energy sea states, neglecting non-linearities leads to overestimation of energy estimates and that the scatter diagram/power matrix approach yields its largest errors in the presence of multi-modal sea states. A similar study is carried out in [12] where the AEP of a point absorber WEC in two deployment sites off the coast of India is computed using power matrices. Finally, the impact of the PTO rating on the overall AEP of a WEC is demonstrated in [13]. As expected, the AEP increases as the PTO rating is increased, and the authors mentions that the PTO rating choice should take into account the wave climate of the potential deployment site. However, only ideal spectral shapes are considered in that study, and the link between spectral shape and PTO rating is not explored. All these previous studies point toward an impact of the resource description on the estimation of WEC power production estimates, and justify further investigation combining more realistic WEC models and detailed long term wave resource data. The present work aims at contributing to this, while bringing the following novelties:

- The WEC numerical model not only includes PTO power capacity capping but also introduces the more complex but more realistic PTO force capping.
- The accuracy (and associated complexity) of the WEC time domain model (accounting for some non-linearities) is combined with a very detailed description of the wave resource (full wave frequency spectra with hourly time resolution) to compute AEPs over the duration of a full year.
- The impact of PTO capping (in terms of power capacity and force) on the performance of different methods of AEP calculations is explored.

- A new metric is introduced to quantified similarity between wave spectra. This metric has been specifically developed for wave energy production applications.

The paper is laid out in the following manner. A concise overview of the modelling of the WEC and the characterisation of the sites are presented in Sections 2 and 3, respectively. The pre-processing of the wave data is described in Section 4 and it is followed by the implementation of PTO simulation with force capping (Section 5). The approaches for the annual energy estimates are detailed in Section 6, including the one recommended by the International Electrotechnical Commission (IEC) [14] and the results of the study with their analysis are given in Section 7, where a new metric is introduced to help investigating how spectral shape similarity impacts AEP error. Section 8 contains a short discussion and the main conclusions.

2. Description of the WEC and its numerical model

The WEC selected for the analysis is a generic version of the device developed by WaveBob Ltd in Ireland [15]. A 1/4*th* scale model of the WaveBob WEC was tested in Galway Bay, Ireland.

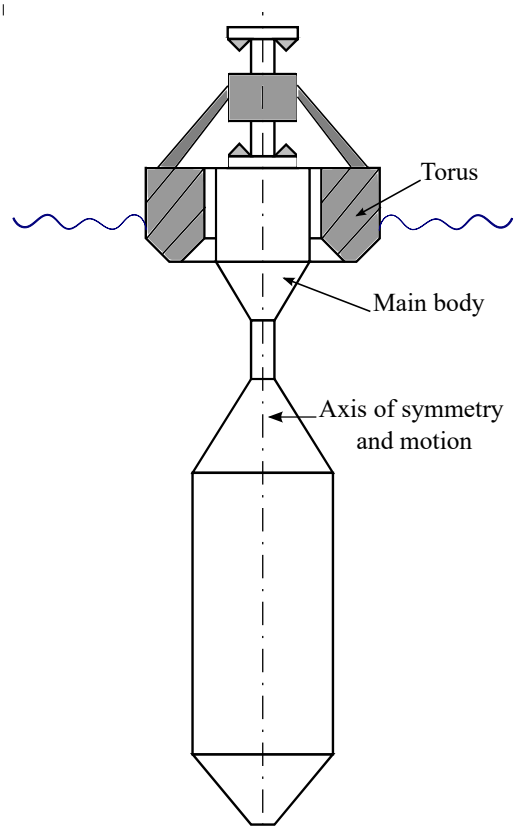

Figure 1: Schematic diagram of the WEC.

The device is an axisymmetric floating two-body heaving absorber, it is self-referenced. The main body is deep, slender and largely submerged, while the other body is a floating torus vertically sliding along the main body's axis (see figure 1). This relative motion between the two bodies drives a hydraulic PTO system. The general characteristics of the system are summarised in Table 1.

Table 1: Parameters of the WEC

Parameter	**Value**
Main body	
Diameter at waterline	8 m
Draft	50 m
Displacement	4680 m^3
Torus	
Outer diameter	20 m
Inner diameter	10 m
Draft	2 m
Stroke length	±4 m
Displacement	278 m^3

The numerical model of the device used in this study is based on what has been developed as part of the NumWEC project [16]. The hydrodynamics relies on the boundary element method (BEM) code Achild3D, developed by the Ecole Centrale Nantes, which runs in time domain. This code assumes infinite water depth, and it is based on linear potential flow theory. The PTO system is modelled as a linear damping mechanism with a stroke limited to ±4 m. In the original version of the code [16], the power capacity of the generator is simulated by a simple cap applied to power production and which therefore does not feed back into the equation of motion of the system. Further code development to simulate a more realistic PTO capping is presented in section 5.1. The mooring system is represented using a linear horizontal spring to simulate a simple slack mooring. Some non-linearities associated with viscosity are also taken into consideration. They were modelled using viscous damping coefficients along the different faces of the device. More details on this and on the verification of the entire numerical model can be found in [16].

3. Site Locations and Wave Resource Data

The available wave energy is site-dependent; therefore, two sites with different wave resource are considered to evaluate the influence of the wave resource description on the power performance of the WEC. The two locations along the Atlantic Coast of Europe are shown in figure 2. The wave climate is considered for the year 2014. Winter 2013-2014 being one of the most energetic winters since 1948 for most of the European Atlantic coasts [17]. Selecting year 2014 as a case study ensures to provide the selected WEC with a wide range of forcing conditions.

Site characterisation is performed through data analysis from two different, but similar hindcast datasets. The French deployment site description is based on the HOMERE public hindcast

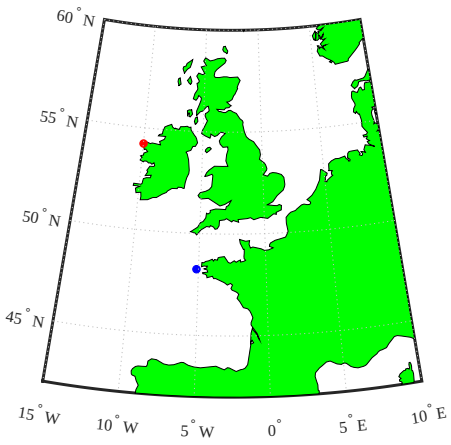

Figure 2: Selected sites: blue point: French site, red point: Irish site

dataset [18] [19], while the Belmullet site representation relies on the ResourceCode wave hindcast, the new extension of HOMERE and the first open access high resolution database covering Western Europe waters [20]. Both hindcast datasets are built around a high-resolution unstructured grid and provide meteo-oceanic conditions from 1993 to 2020. They are generated using the spectral model WaveWatch III developed by the US National Oceanic and Atmospheric Administration (NOAA). HOMERE spans from the Biscay Bay to the channel sea, while ResouceCode is extending from the South of Spain to the Faroe Islands and from the Western Irish continental shelf to the Baltic Sea. Forcing winds are extracted from the CFSR and ERA5 database respectively, while the currents and water levels are accounted for as a forcing conditions on sea states. Those databases both provide integral parameters as well as refined frequency and directional spectra on an hourly basis. For the HOMERE database, the spectra are specified over 32 frequency bins ranging from 0.0373 Hz to 0.7159 Hz and 24 directional bins. For the ResourceCode database, the number of frequency bins has been extended to 36 (from 0.0339 Hz to 0.9527 Hz) and the number of directional bins is also 36. For both databases, the width of the frequency bins is not uniform and is ruled by a geometric progression providing higher resolution at lower frequency. The two databases have been validated, both in terms of integral parameters and of spectral content [18] [21] [20].

The blue dot in figure 2 corresponds to a site located on the West Coast of France, 20 km off the coast of Brittany, and where the average depth is 94 m (latitude: 48.2467°, longitude: −5.1500°). The scatter diagram of the wave resource for this location is presented in figure 3. The red dot marks the location of the Belmullet test site off the West Coast of Ireland, where the average depth is 103 m (latitude: 54.2680°, longitude: −10.2781°). The wave resource at that site is shown in figure 4. Both sites can be considered as deep water sites for the purpose of wave energy extraction by the device considered, which match the hypothesis of the numerical model.

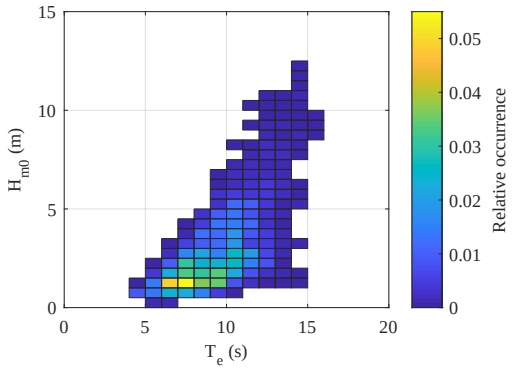

Figure 3: Wave resource of the French site for the year 2014.

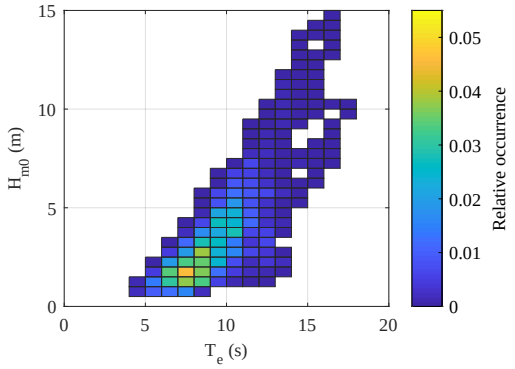

Figure 4: Wave resource of the Irish site for the year 2014.

4. Wave Data Pre-Processing

The raw data from the hindcast database come as spectra and the time domain numerical model requires wave elevation time series as input. There is therefore a need to pre-process the raw hindcast spectral data. This involves the use of the inverse Fourier transform, which requires that the width of the frequency bins of the spectra is uniform. This is however not the case, as mentioned in section 3, and the raw spectra first need to be interpolated with a uniform frequency resolution before the inverse Fourier transform can be applied. More details on this can be found in [4].

A wave elevation time series is generated from a frequency spectrum and a set of random phases. Therefore, an infinite number of time series can be generated from the same spectrum, each of them leading to different power production estimates, because of the non-linearities accounted for in the model. This is particularly the case for the highly-energetic sea states, for which non-linearities are more pronounced. The variability in power production estimates for a given spectrum, from one set of random phases to another, decreases as the time series duration (or repeat period) increases. However, carrying out the WEC time domain simulation over a longer duration requires more computation time, and there is therefore a compromise to be

found between variability and computational burden. This is achieved through a sensitivity analysis carried out for different time series repeat periods associated with a given spectrum. For each repeat period, variability is investigated over 300 realisations (or set of phases). This approach is based on the work of Saulnier et al [22] and it is reported in detail in [4]. The sensitivity analysis was carried out for the most energetic sea state of the Irish site and lead to choosing a repeat period of 1326 s. This simulation duration over the 300 realisations is associated with a mean power production standard deviation of 2.24 % and a maximum error of 5.89 % at the Irish site, while at the French site the standard deviation is of 1.13 % and the maximum error of 3.90 %, which are both deemed acceptable. This repeat period was selected for all the simulations in this study.

5. Power Take-Off System

5.1. PTO Force Capping

The fundamental PTO strategy implemented in the model is damping i.e. the PTO force applied between the two bodies is proportional to the relative velocities between those bodies. However, from an engineering point of view, for a hydraulic PTO, there is an upper limit to the force that the system can apply. In order to simulate this phenomenon, a modification to the original FORTRAN code of the NumWEC project was developed to limit the PTO force. It should be noted, that unlike the simple power capacity capping mentioned in section 2, this adjustment feeds directly into the equation of motion of the system, in other words, the response of the device will be affected.

The force capping consists on imposing a limit when the maximum force that the PTO system can sustain is achieved. When the force required by the linear damping strategy exceeds that maximum allowable PTO force, the force of the PTO system is set to the value of the selected maximum force. The relative motion between the torus and the main body is also limited by a maximum stroke length. When the relative motion between the bodies reaches the lower or higher end stop, an additional restoring force is applied. This force is known as the end stop force (F_{es}), and it is modelled as a very high stiffness (i.e. a force proportional to displacement) but which is only implemented when the stroke exceeds the limit. The capping of the PTO force increases the relative motion compared to a pure uncapped damping and therefore the end stop mechanism is solicited more often. This behaviour can be observed in figure 5.

The application of the end stop force can lead to high-frequency oscillations in the relative motion between the two bodies in the vicinity of the stroke limit, as shown with the red curve of figure 6. Those oscillations are an artefact of the way the end stops are modelled and because of their high-frequency nature, they lead to large velocity and power spikes which are non-physical. It was therefore important to suppress those oscillations, and this was achieved by introducing a damping on top of the high stiffness simulating the end stop. As for the high stiffness, this damping is only applied when the relative motions between the two bodies exceeds the maximum stroke.

The derivation of a suitable damping coefficient is not trivial. Too large a damping causes an over-damping of the whole system, rendering it impossible to restore itself to a normal operating mode afterwards. Too low a damping does not suppress the high frequency oscillations. The damping coefficient was finally tuned empirically i.e. through trial and error, focusing on the

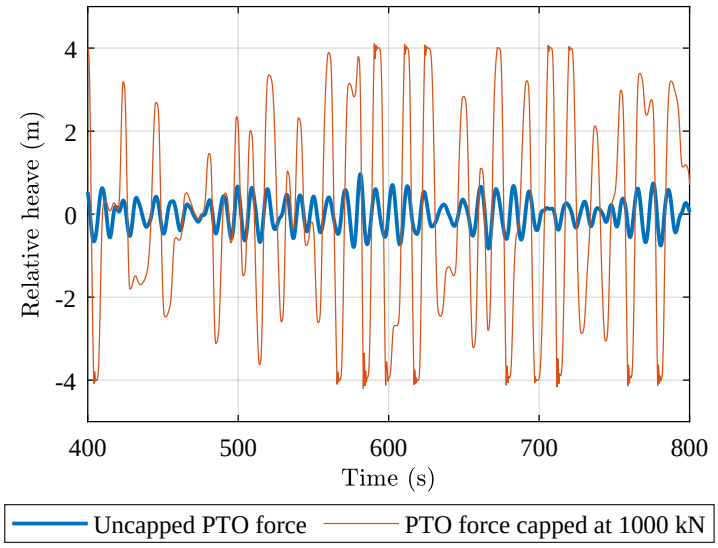

Figure 5: WEC's response in relative heave to PTO force capping

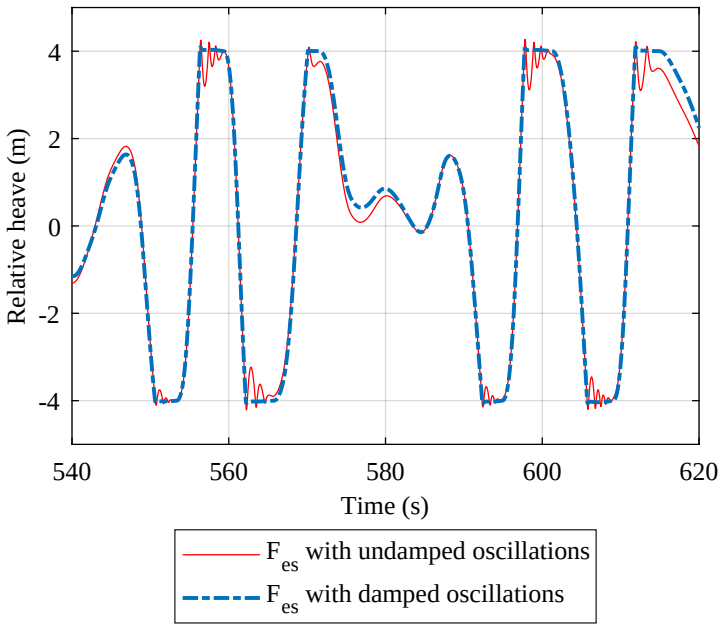

Figure 6: End stop force time series with a damping coefficient of 32 000 kN m^{-1} s. The PTO force is capped at 1000 kN.

most energetic sea states, prone to lead to more "end stop hitting events". The damping coefficient was decreased progressively from an over-damping value until the PTO motion response was affected as little as possible beyond the vicinity of the end of stroke region, while ensuring that the high frequency oscillations at the stroke limits were suppressed. The results of this modification are presented in figure 6. It can be observed that the damping coefficient efficiently removes the oscillations. However, it can also be noticed that the response of the device is sometimes slightly affected at the next wave after the oscillations are damped. It should be noted this empirically derived damping coefficient is kept constant throughout all the simulations carried out for this study.

5.2. PTO Damping Optimisation

To increase the amount of energy captured from the waves, the PTO damping coefficient can be optimised. It should be noted at this stage, to avoid any confusion, that the damping coefficients we are dealing with in this section are unrelated to the damping implemented to simulate the device end stops mentioned in the previous section. The value of the PTO damping coefficient is optimised on a sea state per sea state basis. The optimisation process is based on a JONSWAP spectra ($\gamma = 1$) associated with the integral parameters H_{m0} and T_e corresponding to the centre of each of the bins shown in figures 3 and 4, and it solely focuses on maximising the mean power captured. In other words, for each sea state, the PTO damping selected corresponds to the optimum damping associated with the centre of the bin that the sea state falls in. Finer optimisations of the PTO damping are theoretically possible, especially given that a spectral description of the resource is available. However, it was deemed important to use the same PTO optimisation approach for all the wave resource characterisations considered in section 7 so that the PTO optimisation process does not influence the comparison of energy production estimates between the different sea state characterisations. Moreover, having one optimum PTO setting per H_{m0} - T_e bin is considered more realistic for a real-life device: for a real prototype, this would be realised by obtaining the forecasted H_{m0} and T_e on an half an hour per half an hour basis, and adjust the PTO damping accordingly from a previously estimated map of damping values.

The optimisation itself for a given sea state is based on a brute force approach described in details in [4]. The optimisation process was carried out for the six different test cases detailed in section 6.5 and for all the sea states associated with both sites considered over the year 2014.

6. Mean Annual Energy Production Estimates

In this section, four approaches to compute mean annual energy production estimates are presented:

- Power matrix
- Interpolated power matrix
- Capture length matrix
- Power captures of all the sea states derived directly from the Raw Spectra of the Hindcast Database (RSHD).

The first three methods are based on the WEC's power matrix and will be compared to the fourth one, which will be regarded as the reference approach. It is considered as such because the full spectral information is used to compute the energy production estimates, whereas for the first three methods some of that information is lost as the spectral description is reduced to integral parameters. Further details about each approach are given in the following sections.

6.1. Power Matrix

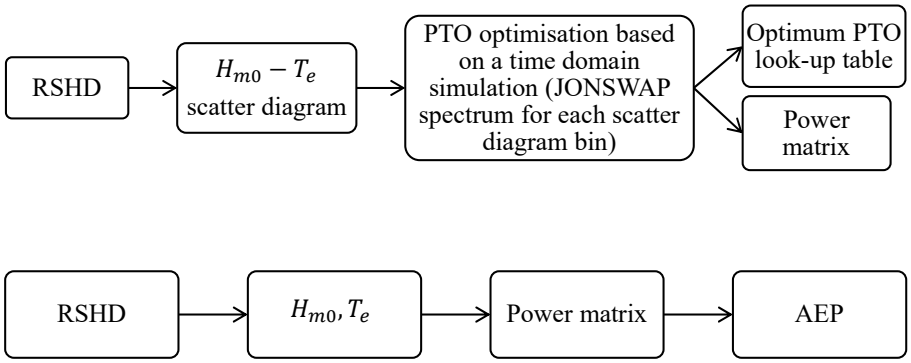

Figure 7: Diagram of the power matrix generation (top), and diagram of the computation of the AEP using the power matrix (bottom).

The power matrix (PM) is the most common representation of how the power capture varies with sea states. In this study, the first step to generate the power matrix of the WEC and the optimum PTO damping look-up table is the derivation of the $H_{m0} - T_e$ scatter diagram through binning (see figure 7) from the RSHD. The bins are 0.5 m in H_{m0} by 1 s in T_e. The second step is the generation of the wave elevation time series of 1326 s (following the sensitivity analysis presented in section 4) for the time domain simulation. For this step, a JONSWAP spectrum ($\gamma = 1$) is produced using the $H_{m0} - T_e$ values corresponding to the centre of each bin of the scatter diagram. Afterwards, the optimum PTO damping coefficient is computed for the centre of each bin of the scatter diagram using the approach described in section 5.2. The output is a table used to look up the PTO optimum damping value of each bin, which is used for the derivation of the power matrix. The resulting power matrix is then directly combined with the site scatter diagram to obtain an estimation of AEP, as shown in figure 7 (bottom).

6.2. Interpolated Power Matrix

The interpolated power matrix (IPM) is a refined version of the method presented in section 6.1. The process to estimate the AEP is the same as that of the power matrix approach, with the additional step of the interpolation of the power matrix at the exact value of H_{m0} and T_e corresponding to each sea state, as illustrated in figure 8.

A linear method was chosen for the interpolation of the power matrix for every combination of $H_{m0} - T_e$. However, when there were no neighbouring bins to provide the necessary points for the interpolation, the queried point took the same value as that of the centre of the bin it falls in.

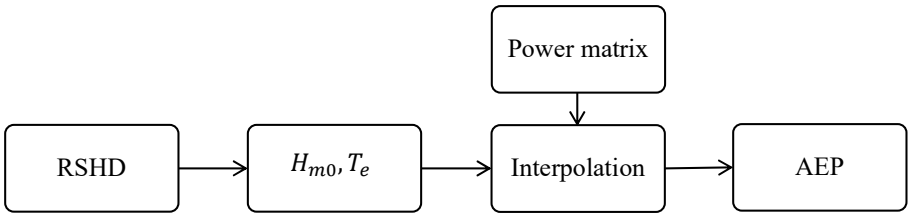

Figure 8: Diagram of the computation of the AEP using an interpolated power matrix.

6.3. Capture Length Matrix

The capture length matrix (CLM) is constructed following the recommendations of the IEC/TS 62600-100 [14]. It can be considered as a power matrix normalised by the incident wave power flux on a cell by cell basis. The dimension of the elements of the capture length matrix is therefore that of a length. The use of a capture length matrix, rather than that of the power matrix, is recommended by the IEC/TS 62600-100 technical specifications because it is less sensitivity to the sea state parameters [14].

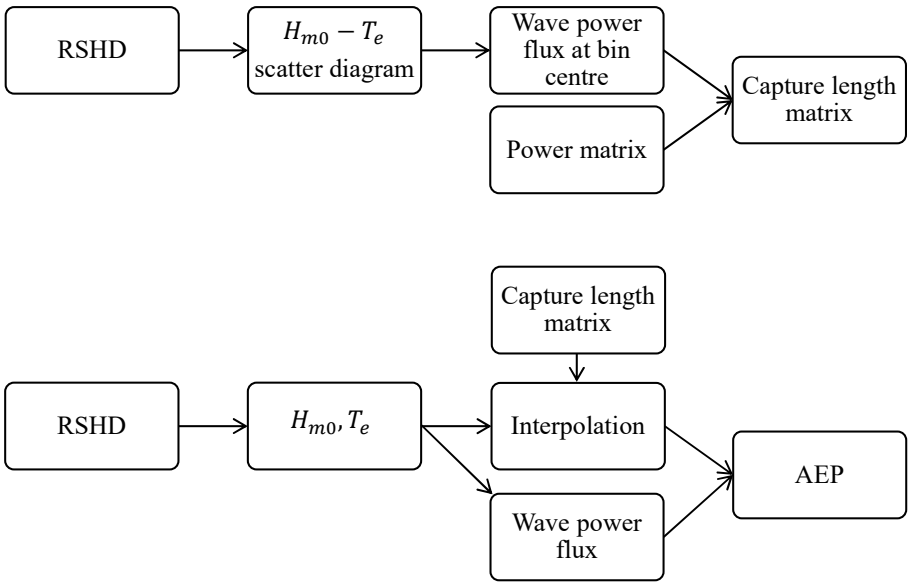

Figure 9: Diagram of the capture length matrix generation (top), and diagram of computation of the AEP (bottom).

The principle for the derivation of the capture length matrix is presented in figure 9 (top). For the estimation of the annual energy production, this matrix was also linearly interpolated, with the same method as the interpolated power matrix. Finally, since the capture length matrix has length dimension, it should be multiplied by the incoming power flux, as shown in figure 9 (bottom). The wave power flux is computed from the exact H_{m0} and T_e values using Equation 1,

where ρ is the density of the water and g is the gravitational acceleration.

$$J = \frac{\rho g^2}{64\pi} H_{m0}^2 T_e \tag{1}$$

6.4. Raw spectra

The last approach considered is the use of the unprocessed data directly from the hindcast database to compute the power production. For each sea state, the H_{m0} and T_e values are calculated to select the right PTO from the PTO damping look-up table obtained while generating the power matrix itself (see figure 10). This method is the most accurate one, as it does not degrade the spectral information to a pair of integral parameters. It is also the most computationally expensive one. It will serve as a reference for the estimation of the annual energy production of the device. The AEP is obtained as the sum of the energy over all the sea states.

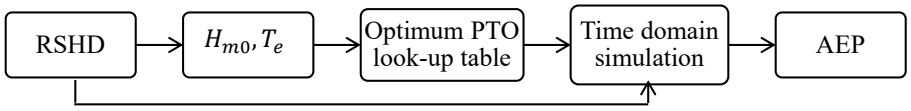

Figure 10: Diagram of computation of the AEP using raw spectra.

6.5. Test Cases

The four methods will be evaluated for the two sites over the full year 2014 and for two different test cases independent of each other: the first one includes three power capacity values (1 MW, 1.5 MW and 3 MW) and no capping of the PTO force; while the second one will comprise three values for the maximum force of the PTO (1 MN, 2 MN and 3 MN) without considering power capacity limits. Although this is not entirely realistic, the deliberate decoupling between these two limits is aimed at better understanding the impact of each type of capping independently.

7. Results and Analysis

Results are presented and analysed in three steps. First, we look how the different energy production estimate methods perform and at how the two PTO capping approaches affect those performances at the global scale of a full year. We then focus on the power matrix approach to analyse in more detail, on the sea state by sea state basis, the distribution of the error in energy production with respect to the reference method, to gain a deeper understanding of those errors. Finally, we investigate the impact that the differences in spectral shapes between the spectra used in the power matrix approach and the exact ones from the hindcast database, have on the error in energy production estimates.

7.1. *Full year analysis*

The overall results for the full year 2014 are presented in figure 11. The energy production of the wave energy converter is presented in the form of the AEP for each case. The three approaches based on power matrices yield very similar results in all cases (the power matrices are presented in appendix, section 9). Compared to the reference data, all three methods overestimate the energy production in the year in question, regardless of the location; however, the level of overestimation is slightly different in each case. In figure 11, we can also see that for a given PTO capping setting, the AEP is always higher for the Irish site than for the French one. This is consistent with the fact that the former is more energetic than the latter, as illustrated in the scatter diagrams of figures 3 and 4. Finally, figure 11 shows that, as expected, for both PTO capping approaches (power capacity and force), the lower the cap, the lower the AEP.

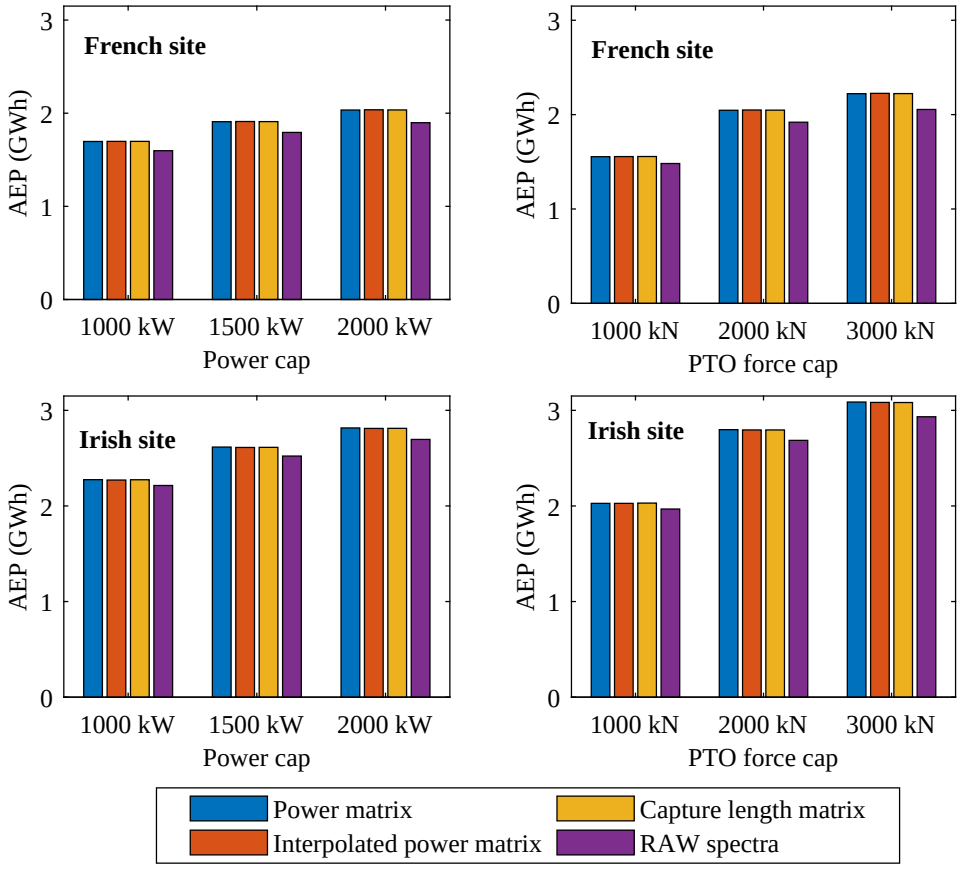

Figure 11: Energy production estimates in 2014 for the two selected sites.

The relative errors in AEP for the three methods with respect to the reference data are tabulated in Table 2. For every configuration and for both sites, the relative errors in AEP are very

Table 2: PTO capping errors of each approach and PTO saturation rate from the raw spectra. $\hat{\epsilon}$ corresponds to relative error in AEP and $\hat{\sigma}$ to normalised standard deviation of the error in AEP.

	Power cap: 1MW				**Power cap: 1.5MW**				**Power cap: 2MW**			
	France		Ireland		France		Ireland		France		Ireland	
Approach	$\hat{\epsilon}$ (%)	$\hat{\sigma}$ (%)	$\hat{\epsilon}$ (%)	$\hat{\sigma}$ (%)	$\hat{\epsilon}$ (%)	$\hat{\sigma}$ (%)	$\hat{\epsilon}$ (%)	$\hat{\sigma}$ (%)	$\hat{\epsilon}$ (%)	$\hat{\sigma}$ (%)	$\hat{\epsilon}$ (%)	$\hat{\sigma}$ (%)
Power matrix	6.22	13.33	2.73	9.29	6.42	14.27	3.72	10.57	7.17	15.35	4.42	11.59
Interpolated power matrix	6.28	10.59	2.57	6.81	6.53	11.46	3.56	7.92	7.30	12.51	4.27	8.79
Capture length matrix	6.28	11.01	2.69	7.05	6.47	11.84	3.61	8.19	7.22	12.88	4.28	9.09
PTO saturation rate (%)	5.56		9.44		3.07		5.16		1.84		3.02	
	PTO force cap: 1MN				**PTO force cap: 2MN**				**PTO force cap: 3MN**			
	France		Ireland		France		Ireland		France		Ireland	
Approach	$\hat{\epsilon}$ (%)	$\hat{\sigma}$ (%)	$\hat{\epsilon}$ (%)	$\hat{\sigma}$ (%)	$\hat{\epsilon}$ (%)	$\hat{\sigma}$ (%)	$\hat{\epsilon}$ (%)	$\hat{\sigma}$ (%)	$\hat{\epsilon}$ (%)	$\hat{\sigma}$ (%)	$\hat{\epsilon}$ (%)	$\hat{\sigma}$ (%)
Power matrix	4.86	10.49	3.01	7.93	6.60	14.20	4.15	10.67	8.14	17.00	5.24	13.05
Interpolated power matrix	4.95	6.83	2.40	7.53	6.75	10.98	4.05	7.42	8.30	13.85	5.12	9.78
Capture length matrix	5.00	7.16	3.11	4.79	6.66	11.34	4.06	7.75	8.19	14.23	5.09	10.12
PTO saturation rate (%)	21.03		26.12		5.83		9.30		1.72		3.12	

similar across the different estimation methods based on matrices, with only at most few tens of percent of difference, which is not significant. Across the different configurations and sites, the relative error (with respect to the benchmark) ranges from 2.4% up to 8.3%. To give some perspective to those numbers, the typical level of availability used for computation of WEC levelised cost of energy (LCOE) is 95% [23], so the level of errors is comparable to the loss due to WEC availability in standard LCOE models. Those levels of error are therefore not negligible, especially the upper half.

Table 2 also shows the standard deviation of the error, which is also normalised by the AEP (as computed by the reference method) and it can be noticed that, in all cases, the normalised standard deviation of the error is higher than the normalised error itself, indicating a significant scatter of the error around its mean value. The tables also contain the mean PTO saturation rate over the full year. For each sea state simulated with the reference method, the saturation rate is defined as the percentage of duration of the simulation time series during which the power generated is equal to the power capacity limit (in the case of power capacity capping) or during which the PTO force is equal to the limit set (in the case of PTO force capping). It can be observed that the lower the power capacity or PTO force cap, the higher the saturation rate.

To visually investigate the impact of PTO power capacity and PTO force capping on AEP estimation errors, figure 12 plots the AEP relative error and normalised standard deviation against the mean PTO saturation rate over the full year. The data plotted in figure 12 are taken from table 2 with the exception of PTO power capacity and force cap values which do not feature in figure 12 to avoid overcrowding. The left column corresponds to PTO power capacity capping, whereas the right column corresponds to PTO force capping. Looking at the top row, which corresponds to the relative error in AEP, we can see that for a given site (indicated by colours) and a given saturation rate, there is little difference in the error value regardless of the method used to compute the energy production estimate (indicated by the different symbols). Looking at the normalised standard deviation of the error (bottom row), the values are higher for the basic power matrix approach compared to the two other approaches involving interpolation, which yield very similar results. This holds true for all cases, except for the one configuration of PTO force capping with the highest saturation rate. We also notice that relative AEP errors and normalised error standard

deviation values are consistently higher for the French site than for the Irish one. The differences between the two cases are potentially explained by further investigation presented in sections 7.2 and 7.3: the caps level are the same for both site, therefore the higher incident power at the Irish site induces higher level of PTO saturation which tends to minimise errors between the methods, and the sea states at the French site are shown to differ more significantly from theoretical JONSWAP than sea states at the Irish site, which will also induce higher differences between the methods. Finally, a key observation which can be made from this figure is that regardless of the site and of the method to compute energy production estimates and even regardless the type of PTO capping considered, both the relative error in AEP and the normalised error standard deviation decrease with increasing PTO saturation rate. This highlights the key impact of PTO saturation rate and therefore of PTO capping setting on those energy production estimate errors.

7.2. Detailed error analysis

Figure 11 shows that there is no significant differences in terms of AEP between the power matrix, interpolated power matrix and capture length matrix approaches. We have therefore decided to focus the detailed error analysis on the power matrix method, as it is the most commonly used approach to estimate WEC energy production. Figures 13 and 14 show the error distribution of the power matrix method with respect to the reference method for all the PTO capping configurations considered and for the French and Irish site respectively. For each of the subplots, the data are plotted against the omnidirectional incoming wave power flux (J) represented with a logarithmic scale on the x-axis. The plots have two y-axes. The right one (in orange) is associated with the histogram showing how the WEC annual energy production is distributed as a function of the incoming wave power flux. This y-axis is in % and is normalised by the AEP. The left y-axis (in blue) corresponds to the error in terms of energy production of the power matrix method with respect to the reference approach. The error (in %) is normalised by the AEP (as predicted by the reference method). Each dot of this scatter plot corresponds to the error associated with one hourly sea state of the year 2014, and it is plotted against the incoming wave power flux (J) associated with that sea state. The colour scales associated with those dots correspond to the saturation rate of the PTO. For the left column, it is the PTO power capacity saturation rate (in %) and for the right column it is the PTO force saturation rate (also in %). The respective colour bars are provided at the bottom of each column, and their respective scale is the same across figures 13 and 14.

Looking at figures 13 and 14, there are some features which are common to all subplots.

- All the point clouds representing the normalised error distribution are skewed towards positive errors, which is consistent with the fact that overall, the power matrix approach overestimates AEPs as shown in figure 11.
- For low values of incoming wave power ($J < 5\,\mathrm{kW\,m^{-1}}$) the normalised error values are small (typically less than 10%). This is due to the fact that in those low energy sea states, little energy is produced by the WEC and so the absolute error between the power matrix approach and the reference method is small compared to the AEP. Hence, the low normalised error values observed. However, in this range of wave energy flux, as can be seen from the histograms, only a small portion ($< 3\%$) of the overall AEP is produced and so this relatively low level of error has little impact on the overall AEP error.

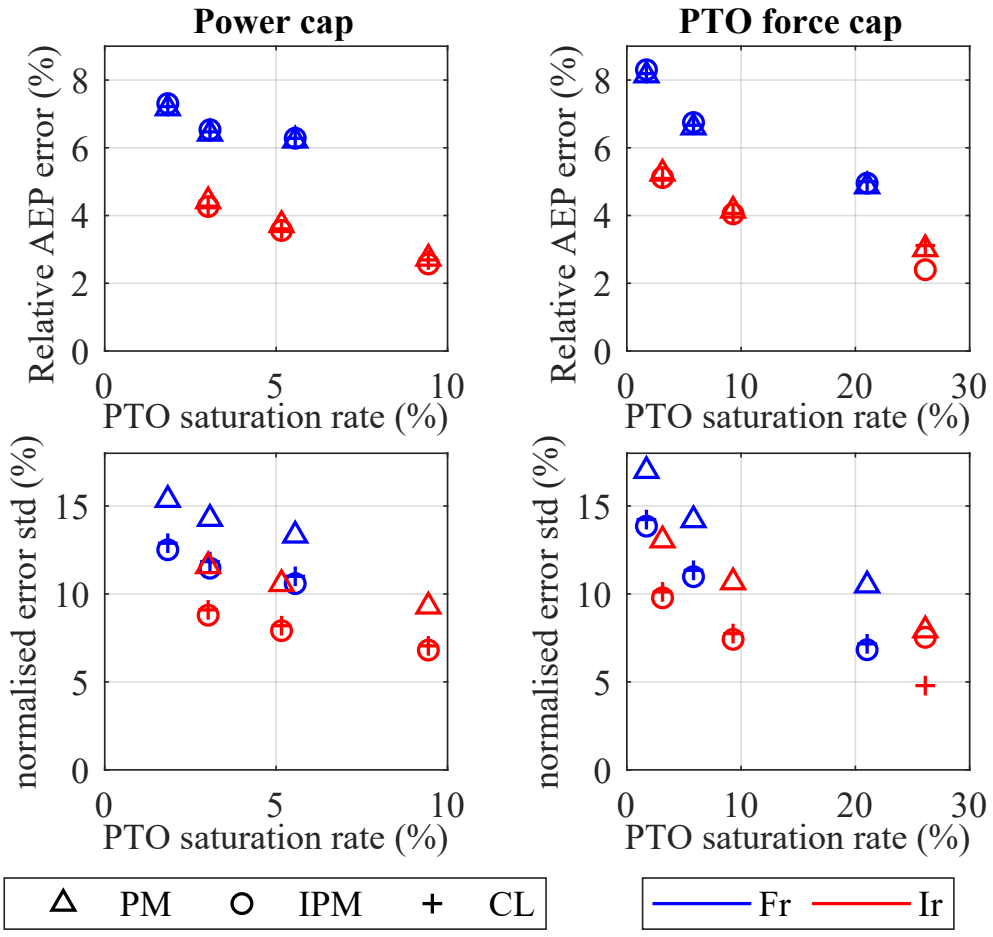

Figure 12: Error versus PTO saturation. The top row corresponds to relative error in AEP and the bottom row to normalised standard deviation of the error in AEP. The left column corresponds to PTO power capacity capping and the right column to PTO force capping. Each symbol corresponds to a method for computing the energy production estimates, as indicated in the bottom left legend with PM: power matrix, IPM: interpolated power matrix and CL: capture length matrix. Blue corresponds to the French site (Fr) and red to the Irish (Ir) one, as indicated in the bottom right legend.

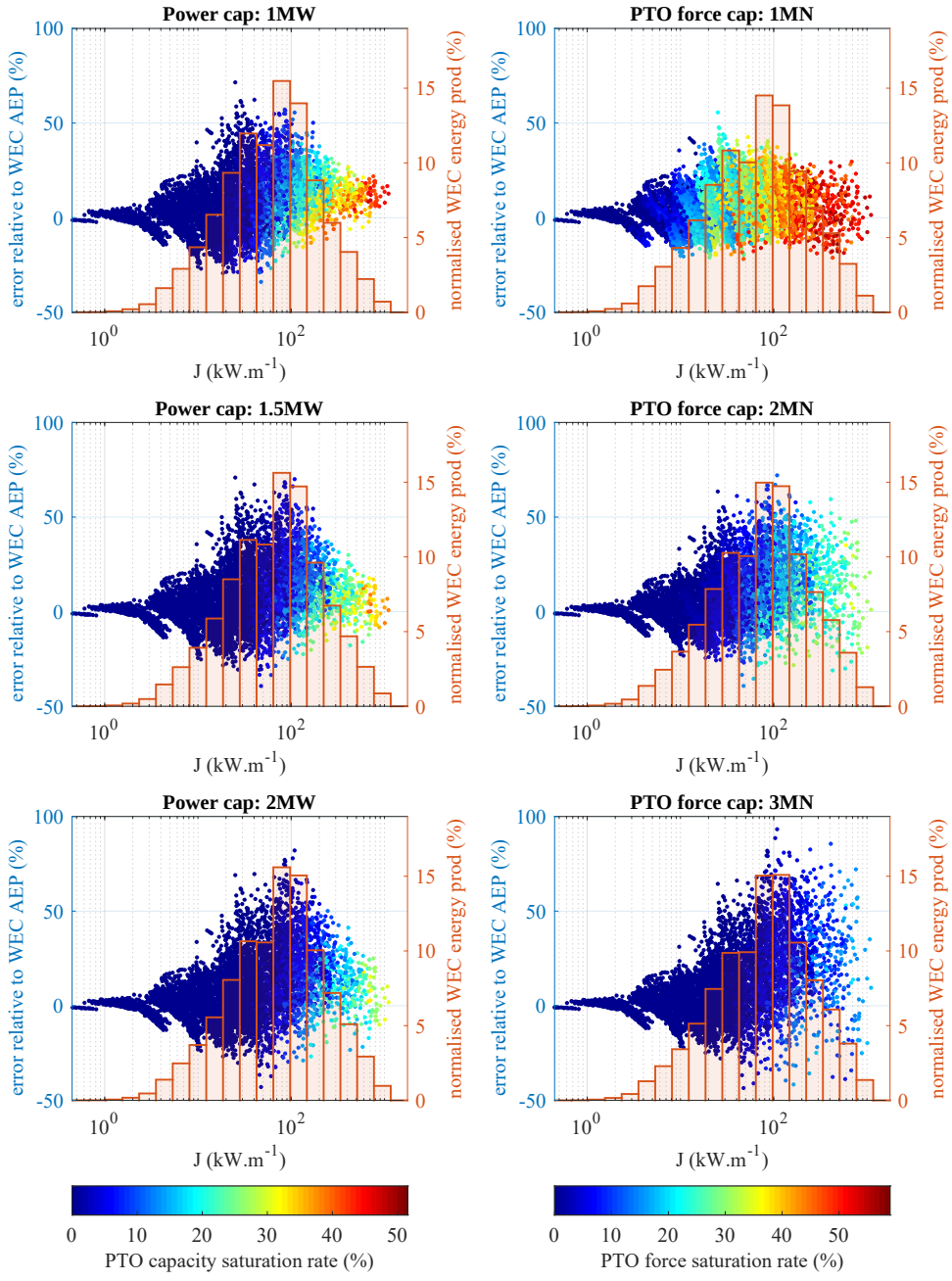

Figure 13: Energy production estimate error of the power matrix method with respect to the reference approach, for every sea state of the year 2014 at the French site (left y-axis) as a function of omnidirectional wave power flux (x-axis). The error is normalised by the AEP. The right y-axis is associated with the histogram of the WEC energy production distribution as a function of the wave power flux. Each subplot corresponds to different PTO capping process and value.

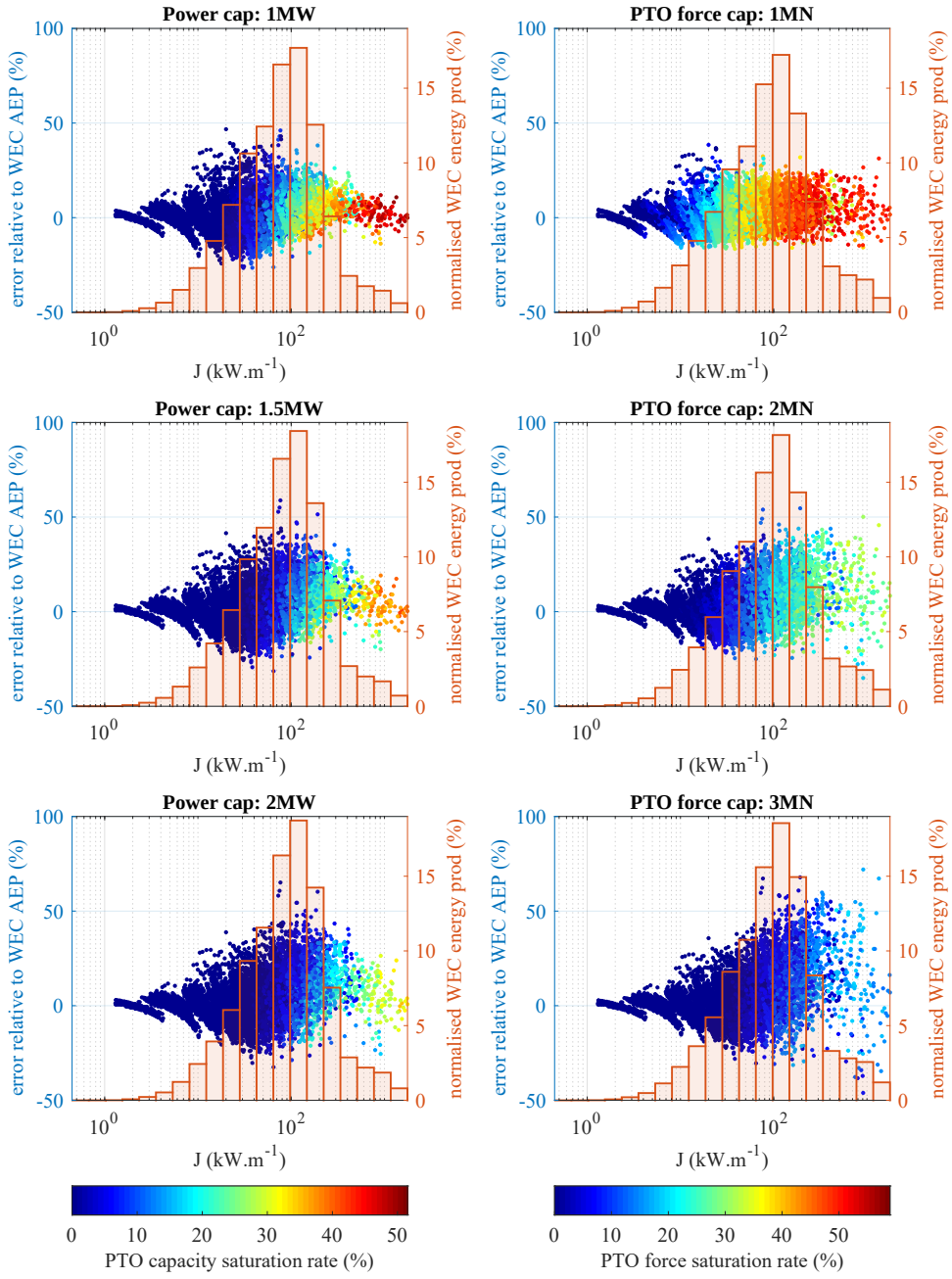

Figure 14: Energy production estimate error of the power matrix method with respect to the reference approach, for every sea state of the year 2014 at the Irish site (left y-axis) as a function of omnidirectional wave power flux (x-axis). The error is normalised by the AEP. The right y-axis is associated with the histogram of the WEC energy production distribution as a function of the wave power flux. Each subplot corresponds to different PTO capping process and value.

- PTO saturation rates (as indicated by the colour of the points of the scatter plots) increase with J. This is to be expected because the PTO is more likely to be saturated in more energetic sea states.
- Levels of PTO saturation (power capacity and force) increase with decreasing capping levels. This can be seen from the number of points associated with higher PTO saturation rates increasing as capping levels decrease. This is consistent with the full year statistics discussed in section 7.1.

Focusing on the power capacity capping subplots (left column), we can see that the spread of the relative error increases with J, but only until the PTO saturation rate reaches values of around 15%. As this rate increases with increasing values of J, the spread of the relative error plateaus and then starts to decrease. The rate of decrease depends on the power capacity cap value and the lower it is, the higher the rate of decrease. We also notice on the lowest power capacity cap subplots that the points associated with the highest PTO saturation rate exhibit some of the lowest AEP relative errors for energetic sea states. To try to find a possible interpretation for this phenomenon, let us consider the PTO power generation timeseries in a highly energetic sea state for which PTO power capacity saturation rate is high. In this situation, the power generation timeseries will be at the power capacity cap value for a significant amount of time. This "capping process" is likely to make the average power generation less sensitive to the spectral shape of different sea states equally highly energetic. This would explain the decreasing level of AEP relative errors as power capacity saturation increases. In the case of PTO force capping, we observe a similar trend of increasing scatter of the relative AEP error with J, but this increase stops for PTO saturation rates of around 20% whereas it is 15% for PTO capacity saturation rate. The other notable difference with power capacity capping is that beyond this level of PTO saturation, the spread of the AEP relative error does not decrease as J increases, but rather plateaus. The implications of PTO force capping on power generation are less direct than those of PTO power capacity capping and we therefore have no obvious interpretation for this "plateauing effect". Nevertheless, the observations made for both PTO capping processes highlight again the important impact of PTO saturation (in terms of power capacity and force) on the AEP error.

The energy production histograms make it possible to relate the distribution of the relative AEP error as a function of energy production. For the French site, we can see on figure 13 that about 50% of the AEP is produced in sea states whose energy flux lies between $28\,\mathrm{kW\,m^{-1}}$ and $147\,\mathrm{kW\,m^{-1}}$ and that this range of energy flux is also where the AEP relative error is the highest for the configuration where the PTO is capped in terms of power capacity. For the Irish site (figure 14), we can see that the histograms are more peaky than for the French site and that the majority of the AEP is produced in slightly more energetic sea states.

7.3. Spectral shape and AEP error

Several articles in the literature [11, 9] suggest that the error in AEP between a power matrix approach and one based on exact spectra is strongly influenced by the difference in spectral shape between the actual spectra and the standard fitted spectra used for the power matrix calculations. To investigate how this applies to our case studies, we introduce a metric designed to quantify the difference in spectral shape between two spectra in terms of wave energy flux. This approach is motivated by the fact that the wave energy flux corresponds to the available power for wave energy conversion at a given site.

Starting with the omnidirectional spectral density function $S(f)$, as defined in [24, chapter 2], where f is the wave frequency, the wave energy flux associated with this omnidirectional spectrum can be calculated as follows:

$$J = \frac{\rho g^2}{4\pi} \int \frac{S(f)}{f} df \tag{2}$$

discretising (2):

$$J = \frac{\rho g^2}{4\pi} \sum_k \frac{S_k}{f_k} \Delta f_k \tag{3}$$

where S_k is the omnidirectional spectral density of the k^{th} bin of the spectrum, whose bin width is Δf_k and central bin frequency is f_k. We then define J_k as the omnidirectional wave energy flux associated with the k^{th} bin of the spectrum:

$$J_k = \frac{\rho g^2}{4\pi} \frac{S_k}{f_k} \Delta f_k \tag{4}$$

Considering a spectrum S_a to be compared to a reference spectrum S_b in terms of wave energy flux, the metric we propose, noted ϵ_J and based on the normalised root mean square error concept is defined by:

$$\epsilon_J = \sqrt{\frac{\sum_k \left(J_{a_k} - J_{b_k}\right)^2}{\sum_k \left(J_{b_k}\right)^2}} = \sqrt{\frac{\sum_k \left(\frac{S_{a_k} - S_{b_k}}{f_k} \Delta f_k\right)^2}{\sum_k \left(\frac{S_{b_k}}{f_k} \Delta f_k\right)^2}} \tag{5}$$

where J_{a_k} and J_{b_k} are the omnidirectional wave energy flux associated with the k^{th} bin of the S_a and S_b spectra respectively. Similarly, S_{a_k} and S_{b_k} are the omnidirectional spectral density of the k^{th} bin of the S_a and S_b spectra, respectively. With Δf_k uniform, (5) becomes:

$$\epsilon_J = \sqrt{\frac{\sum_k \left(J_{a_k} - J_{b_k}\right)^2}{\sum_k \left(J_{b_k}\right)^2}} = \sqrt{\frac{\sum_k \left(\frac{S_{a_k} - S_{b_k}}{f_k}\right)^2}{\sum_k \left(\frac{S_{b_k}}{f_k}\right)^2}} \tag{6}$$

Qualitatively, the smaller ϵ_J is the more the shapes of S_a and S_b are similar and conversely, with $\epsilon_J = 0$ corresponding to $S_a = S_b$.

Figure 15 shows the error ϵ_J of the spectra used in the power matrix approach (as detailed in section 6.1) with respect to the corresponding exact spectra. The plots cover the full 2014 year, with each dot corresponding to an hourly sea state. ϵ_J is plotted against the sea state's wave energy flux, represented on a logarithmic scale. We can see on the figure that for both sites, the value of ϵ_J and its spreading decreases as J increases. Physically, this means that the more energetic the sea state is, the closer its spectral shape is to a uni-modal JONSWAP spectrum. Conversely, the larger values of ϵ_J observed for low energy sea states suggest an increased predominance of multimodal spectra, for which a JONSWAP fit is less appropriate. Over the full range of energy flux, we observe that the spread in ϵ_J is lower for the Irish site than for the French one. This suggests that the shape of the spectra encountered at the Irish site are "closer"

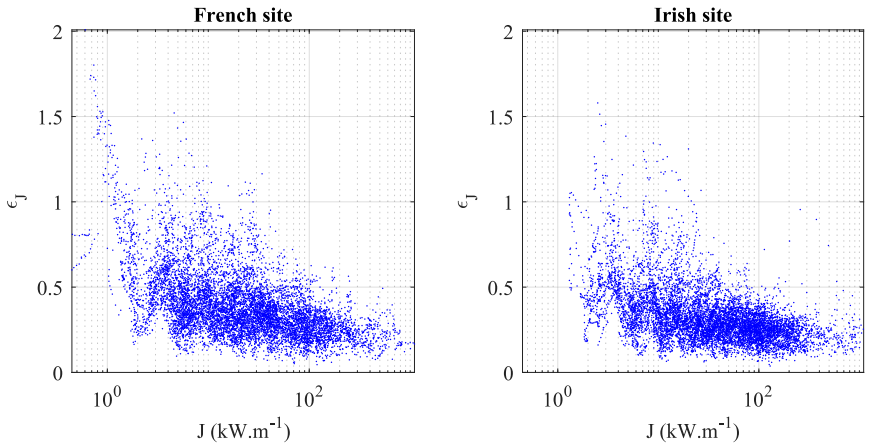

Figure 15: ϵ_J error values for the spectra used for the power matrix approach with respect to the exact spectra plotted against wave energy flux J, for the year 2014, for both sites considered. Each dot corresponds to an hourly sea state.

to JONSWAP spectra than it is the case for the French site.

The normalised AEP errors values shown on figures 16 and 17 are the same as for figures 13 and 14 but this time they are plotted against ϵ_J, represented on the x-axis with a log scale. As for figures 13 and 14, the colour of each dot corresponds to the PTO power capacity saturation rate for the left column and to the PTO force saturation rate for the right column. Figure 16 corresponds to the French site and figure 17 the Irish site.

For all subplots of figures 16 and 17, and for $\epsilon_J < 0.4$, there is a clear correlation between AEP normalised error and ϵ_J, with the AEP error spread decreasing with decreasing values of ϵ_J. This correlation is more pronounced for the PTO power capacity capping configurations than for the PTO force capping configurations. For $\epsilon_J > 0.4$, there is less of a correlation, and we notice low AEP errors for the highest values of ϵ_J. However, the colour of those dots indicate that they are associated with low saturation rates and therefore, as seen in figure 13 and 14, with low energy sea states. Those low AEP error values for high ϵ_J can therefore be explained by the normalisation process involved in the AEP error computation.

Overall, the results plotted in figures 16 and 17 confirm the impact of spectral shape similarity on the error in AEP between the power matrix approach and the method based on the exact spectra. More specifically, they show that to a large extent, the more similar the shape of the exact spectra and that of the fitted spectra used in the power matrix approach, the lower the error.

8. Conclusions

8.1. General Conclusions

In this study, four different approaches were explored to investigate the influence of the wave resource description on the prediction of the power production of a wave energy converter during the year 2014 at two sites, located off the West coast of France and Ireland. The four methods

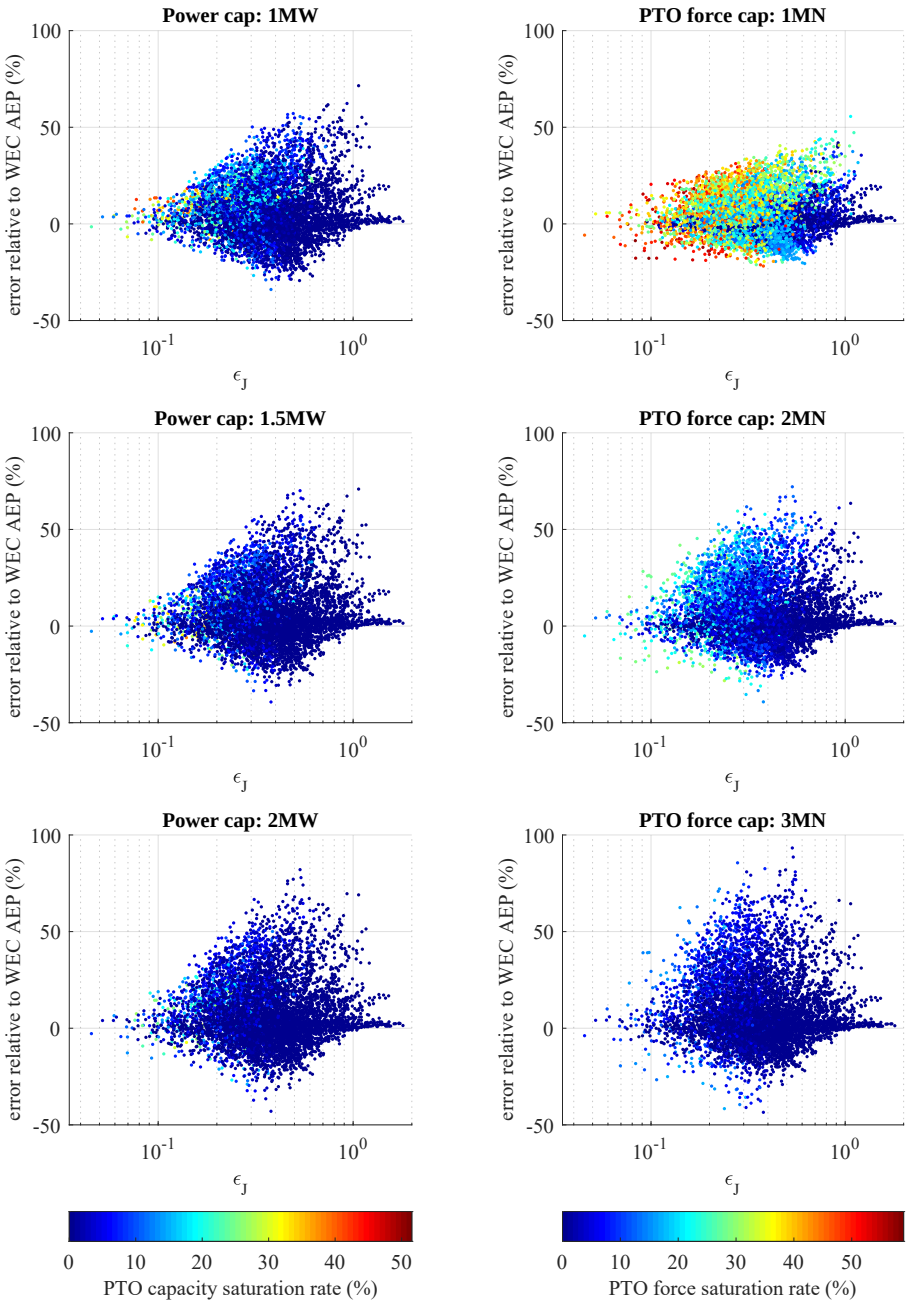

Figure 16: Energy production estimate error of the power matrix method with respect to the reference approach, for every sea state of the year 2014 at the French site as a function of ϵ_J. The error is normalised by the AEP. Each subplot corresponds to different PTO capping process and value.

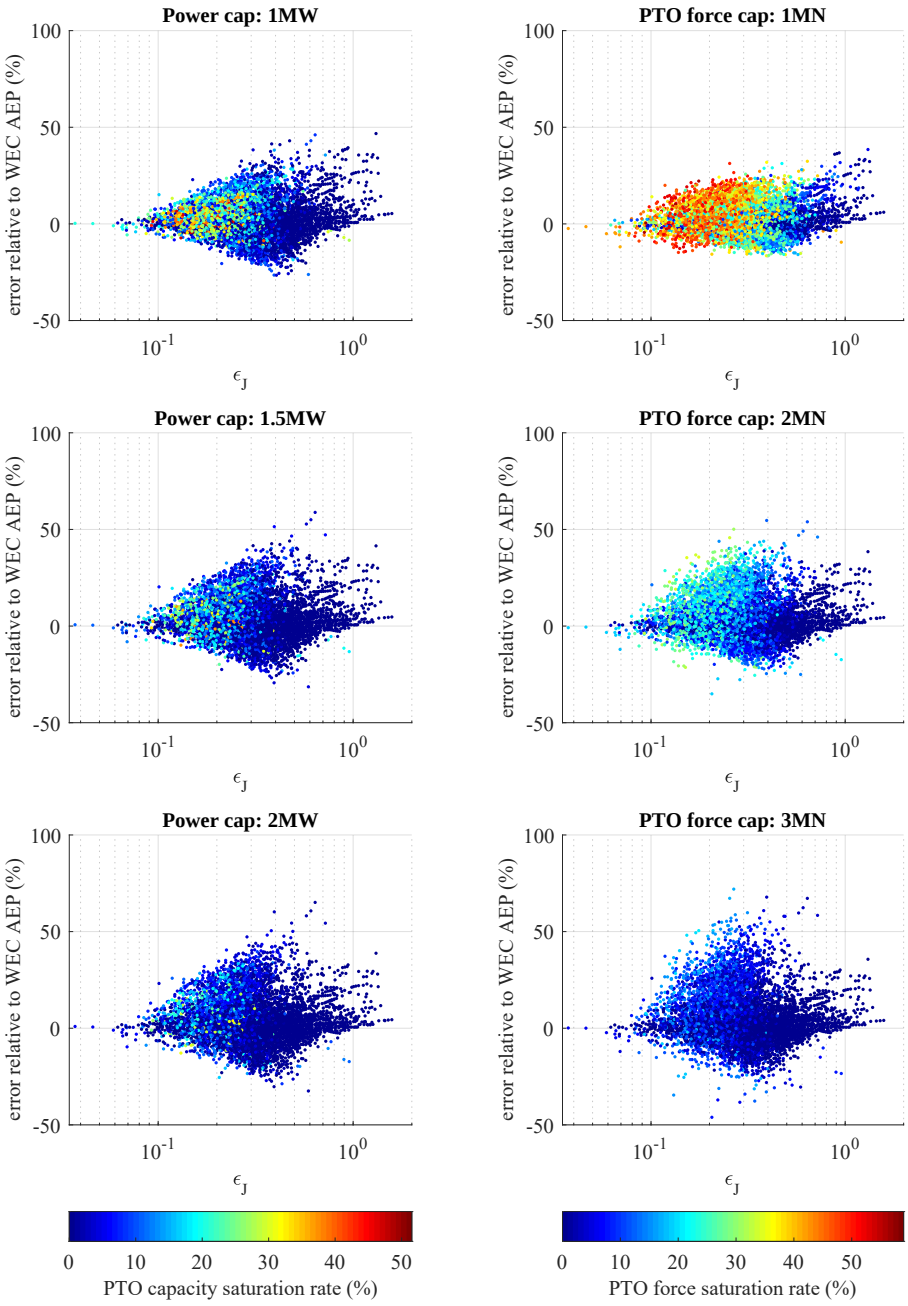

Figure 17: Energy production estimate error of the power matrix method with respect to the reference approach, for every sea state of the year 2014 at the Irish site as a function of ϵ_J. The error is normalised by the AEP. Each subplot corresponds to different PTO capping process and value.

are based on the use of a power matrix, an interpolated power matrix, a capture length matrix, and raw spectral data, the latter being considered as the reference method. The estimations of the performance were carried out using a time-domain numerical model which accounted for the non-linearities associated with viscous damping on the WEC body and PTO end-stop phenomena. The study also introduced two different ways to account for PTO capping: a simple PTO power capacity capping and a more realistic PTO force capping. Although for a real full-scale device, both capping approaches would exist concurrently, it was decided in this study to investigate them separately in order to better identify their respective influence independently.

In this study, the relative error in AEP for the power matrix with respect to the approach relying on raw spectra tend to be smaller than what was reported in previous studies. For example, in [9], the production estimate error ranges from -7% to -44%, depending on the type of WEC and site considered. In [11], the error ranges from 7% to 20%, also depending on the type of WEC and site considered. For comparison, in our study the error ranges from 3% to 8% depending on the site and on the PTO capping configuration. It is interesting to note that in [9], the numerical model used relies on a linear frequency domain approach which does not account for non-linearities associated with viscosity, end stop and PTO capping. In [11], the results mentioned above correspond to a model with a similar PTO damping strategy as the one implemented in our study and which accounts for the non-linearities associated with viscosity however, it does not account for PTO capping. Although those different studies (including ours) are associated with different WECs, different sites and different time periods, they suggest that the level of fidelity in the models used in the studies has a significant impact on the results. More specifically, our study shows that although, as suggested by prior studies, the similarity in spectral shapes between the spectra used for the power matrix method and the exact ones has a significant impact on the error, so does the PTO capping. Indeed, our study shows that, independently of spectral shape similarities, there is a clear correlation between PTO capping (and therefore PTO saturation rate) and error in energy production estimates based on the power matrix method: the lower the PTO capping, the higher the PTO saturation rate and the lower the error. For example, for the French site, the relative error in AEP from the "matrix based" approaches relative to the benchmark computations drops from 8% to just under 5% as the PTO force saturation rate increases from 2% to 21% (see figure 12). This strongly suggests that PTO capping should be taken into consideration for meaningful estimates of WEC energy production.

The investigation of the impact of spectral shape similarities between the spectra used in the power matrix method and the raw spectra has led to the development of a new metric (noted ϵ_J) to compare spectral shapes in terms of wave energy flux. Using this metric, we have confirmed that spectral shape similarities play a role in AEP error, but we have also found out that for the two sites considered in our case study, the exact spectra of the most energetic sea states can be better approximated by standard JONSWAP spectra than it is the case for the low energy sea states.

Finally, this study shows that, considered independently, both PTO power capacity capping and PTO force capping have the same qualitative impact on AEP errors, with the error going down with PTO cap values. However, when looking at the results on a sea state per sea state basis, the way the error is affected by those two capping approaches independently is clearly different (see figures 13 and 14). Given that they both correspond to two different physical limits of a PTO system, they should ideally, in the future, both be accounted for simultaneously in

simulations.

8.2. Implications for Wider Wave Energy Sector Stakeholders

The study shows that in terms of AEP error, there is very little difference between the power matrix, interpolated power matrix and capture length matrix methods with respect to the benchmark reference method. Indeed, the differences in AEP estimates between the different "matrix based" methods are only at most a few tenths of percent (see table 2). Our case study therefore does not support the IEC technical specifications [14] recommending the use of capture length matrix rather than power matrix. We suggest that the technical committee editing the technical specification should consider in future editions to allow the use of either the capture length matrix or power matrix. It should be nevertheless highlighted that the results of this study are likely to be, to some extent, specific to the WEC and site considered and that broader studies are required to provide a definitive answer on that question.

It should be also noted that although the relative error in AEP computed in the study are only single digit percentages, this should not hide the fact that on a sea state per sea state basis, the spread of that error is significant and for some individual sea states, the error in energy production estimates can be as high as 90% of the AEP for the power matrix approach (see figure 13). Using a method relying on matrix interpolation reduces that spread, as seen in table 2, compared to the basic power matrix approach.

CRediT authorship contribution statement

Lissie M. de la Torre-Castro: Conceptualisation, Methodology, Formal analysis, Writing - original draft, Visualisation. **Rémy C.R. Pascal:** Conceptualisation, Methodology, Formal analysis, Writing - review and editing. **Yves Pérignon:** Writing - original draft, Project administration, Funding acquisition. **Aurélien Babarit:** Methodology, Software, Writing - review and editing. **Grégory S. Payne:** Conceptualisation, Methodology, Formal analysis, Writing - original draft, Writing - review and editing, Visualisation, Supervision.

Declaration of competing interest

The authors declare that they have no known competing financial interests or personal relationships that could have appeared to influence the work reported in this paper.

Acknowledgements

G.S. Payne and Y. Pérignon's work was carried out within the framework of the WEAMEC, West Atlantic Marine Energy Community, and with funding from the Pays de la Loire Region and Europe (European Regional Development Fund) through the RC+ project. L. de la Torre's work was carried out during her master thesis of the Erasmus Mundus Joint Master Degree in Renewable Energy in the Marine Environment, which was financed by the European Commission - Education, Audiovisual and Culture Executive Agency (EACEA).

9. Appendix

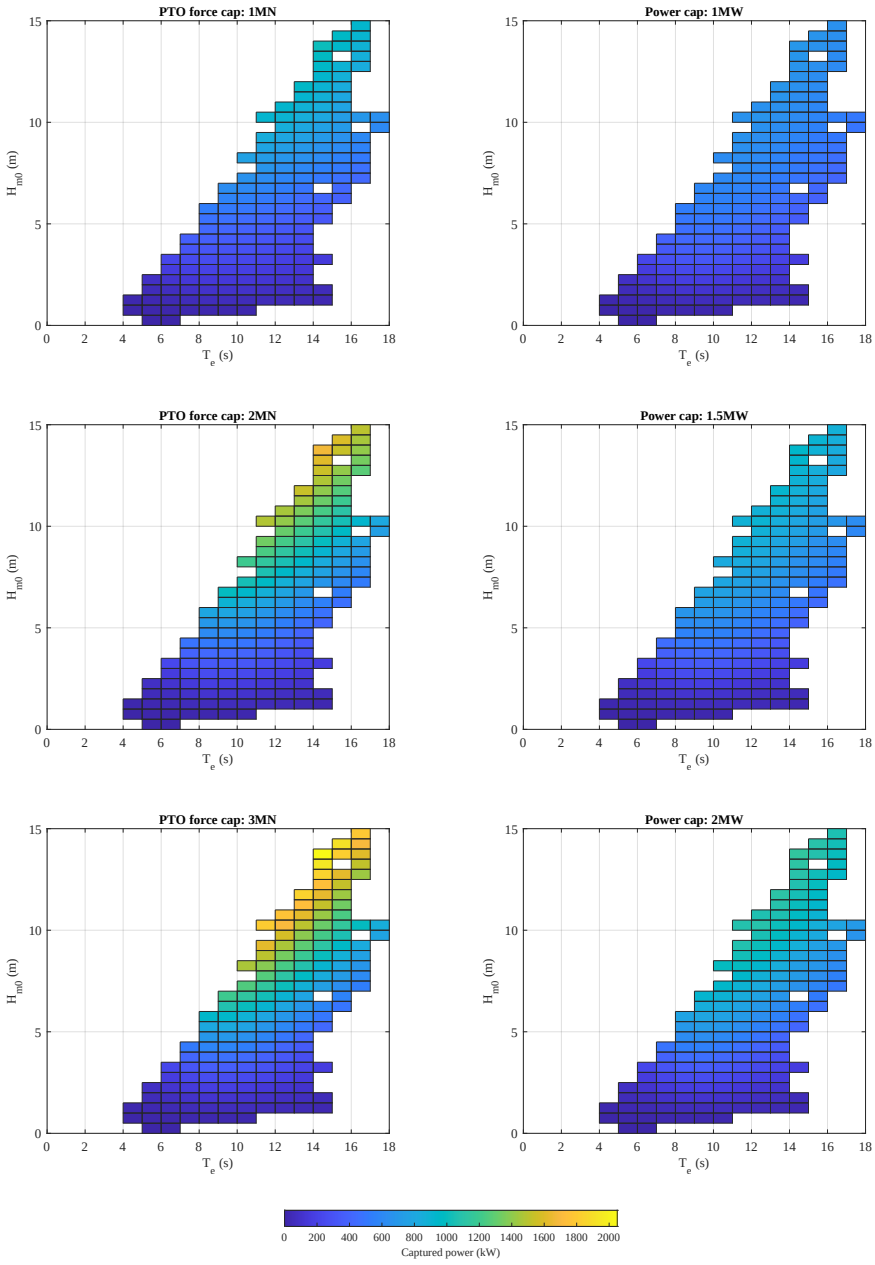

Figure 18: WEC power matrix for each PTO capping process and value.

References

[1] K. Gunn, C. Stock-Williams, Quantifying the global wave power resource, Renewable Energy 44 (2012) 296–304. doi:10.1016/J.RENENE.2012.01.101.

[2] A. Babarit, J. Hals, M. J. Muliawan, A. Kurniawan, T. Moan, J. Krokstad, Numerical benchmarking study of a selection of wave energy converters, Renewable Energy 41 (2012) 44–63. doi:10.1016/J.RENENE.2011.10.002.

[3] R. C. R. Pascal, F. Gorintin, G. S. Payne, D. Darbinyan, Y. Pérignon, Influence of resource definition on defining a wec optimal size, in: Proceedings of the 13th European Wave and Tidal Energy Conference, Naples, Italy, 2019.

[4] G. S. Payne, R. C. R. Pascal, A. Babarit, Y. Perignon, Impact of wave resource description on wec energy production estimates, in: Proceedings of the 14th European Wave and Tidal Energy Conference, Plymouth, UK, 2021.

[5] B. Holmes, S. Barrett, Sea & swell spectra, in: Proceedings of the 7th European Wave and Tidal Energy Conference, Porto, Portugal, 2007.

[6] G. Nolan, J. V. Ringwood, B. Holmes, Short term wave energy variability off the west coast of ireland, in: Proceedings of the 7th European Wave and Tidal Energy Conference, Porto, Portugal, 2007.

[7] S. Barrett, B. Holmes, A. Lewis, Monitoring of seaway variability on wec performance, in: Proceedings of the 2nd International Conference on Ocean Energy, Brest, France, 2008, pp. 1–9.

[8] M.-A. Kerbiriou, M. Prevosto, C. Maisondieu, A. Clement, A. Babarit, Influence of sea-states description on wave energy production assessment, in: Proceedings of the 7th European Wave and Tidal Energy Conference, Porto, Portugal, 2007.

[9] A. D. de Andrés, R. Guanche, J. Weber, R. Costello, Finding gaps on power production assessment on wecs: Wave definition analysis, Renewable Energy 83 (2015) 171–187. doi:10.1016/J.RENENE.2015.04.026.

[10] C. Maisondieu, M. L. Boulluec, Benefits of using a spectral hindcast database for wave power extraction assessment, The International Journal of Ocean and Climate Systems 7 (2016) 83–87, number: 3. doi:10.1177/1759313116649967.

[11] A. Mérigaud, J. V. Ringwood, Power production assessment for wave energy converters: Overcoming the perils of the power matrix, Proceedings of the Institution of Mechanical Engineers Part M: Journal of Engineering for the Maritime Environment 232 (2018) 50–70. doi:10.1177/1475090217731671.

[12] S. Chandrasekaran, V. Sricharan, Numerical study of bean-float wave energy converter with float number parametrization using wec-sim in regular waves with the levelized cost of electricity assessment for indian sea states, Ocean Engineering 237 (2021) 109591. doi:https://doi.org/10.1016/j.oceaneng.2021.109591.
URL https://www.sciencedirect.com/science/article/pii/S0029801821009768

[13] A. F. Falcão, J. C. Henriques, L. M. Gato, Rotational speed control and electrical rated power of an oscillating-water-column wave energy converter, Energy 120 (2017) 253–261. doi:10.1016/j.energy.2016.11.078.

[14] International Electrotechnical Commission, Marine energy – Wave, tidal and other water current converters – Part 100: Electricity producing wave energy converters – Power performance assessment (IEC TS 62600-100:2012) (2012).

[15] J. Weber, F. Mouwen, A. Parish, D. Robertson, Wavebob – Research Development Network and Tools in the Context of Systems Engineering, in: Proceedings of the 8th European Wave and Tidal Energy Conference, Uppsala, Sweden, 2009, pp. 416–420.

[16] A. Babarit, J. Hals, A. Kurniawan, M. Muliawan, T. Moan, J. Krokstad, The NumWEC project: numerical estimation of energy delivery from a selection of wave energy converters, 2011.

[17] G. Masselink, B. Castelle, T. Scott, G. Dodet, S. Suanez, D. Jackson, F. Floc'h, Extreme wave activity during 2013/2014 winter and morphological impacts along the atlantic coast of europe, Geophysical Research Letters 43 (5) (2016) 2135–2143. doi:10.1002/2015GL067492.

[18] E. Boudière, C. Maisondieu, F. Ardhuin, M. Accensi, L. Pineau-Guillou, J. Lepesqueur, A suitable metocean hindcast database for the design of Marine energy converters, International Journal of Marine Energy 3-4 (2013). doi:10.1016/j.ijome.2013.11.010.

[19] M. Accensi, C. Maisondieu, Homere, Tech. rep. (2015). doi:http://dx.doi.org/10.12770/cf47e08d-1455-4254-955e-d66225c9dc90.

[20] M. Accensi, M. Alday, C. Maisondieu, N. Raillard, D. Darbynian, C. Old, B. Sellar, O. Thilleul, Y. Pérignon, G. S. Payne, L. O'boyle, L. Fernandez, F. Dias, R. Chumbinho, G. Guitton, ResourceCODE framework: A high-resolution wave parameter dataset for the European Shelf and analysis toolbox, in: Proceedings of 14th European Wave and Tidal Energy Conference, Plymouth, UK, 2021.

[21] Y. Perignon, C. Maisondieu, Assessing accuracy of hindcast spectral content in the estimation of wave energy resource, in: Proceedings of the 12th European Wave and Tidal Energy Conference, Cork, Ireland, 2017.

[22] J.-B. Saulnier, P. Ricci, A. H. Clément, A. F. D. O. Falcão, Mean power output estimation of wecs in simulated sea, in: Proceedings of the 8th European Wave and Tidal Energy Conference, 2009, pp. 891–900.

[23] R. Guanche, A. De Andrés, I. J. Losada, C. Vidal, A global analysis of the operation and main-

tenance role on the placing of wave energy farms, Energy Conversion and Management (2015) 440–456doi:10.1016/j.enconman.2015.09.022.
[24] M. Tucker, E. Pitt, Waves in Ocean Engineering, Elsevier, 2001.